PROCEEDINGS OF SCIENCE

The MTV Experiment: from T Violation To Lorentz Violation

J. Murata[*1], **H. Baba**[2], **J.A. Behr**[3], **F. Goto**[4], **S. Inaba**[1], **H. Kawamura**[5], **M. Kitaguchi**[4], **C.D.P Levy**[3], **H. Masuda**[1], **Y. Nakaya**[1], **K. Ninomiya**[1], **J. Onishi**[1], **R. Openshaw**[3], **S. Ozaki**[1], **M. Pearson**[3], **Y. Sakamoto**[1], **H. Shimizu**[4], **Y. Shimizu**[1], **S. Tanaka**[1], **Y. Tanaka**[1], **R. Tanuma**[1], **Y. Totsuka**[1], **E. Watanabe**[1], **M. Yokohashi**[4]

[1] *Department of Physics, Rikkyo University, Tokyo 171-8501, Japan*
[2] *Nishina Center, RIKEN, Saitama 351-0198, Japan*
[3] *TRIUMF, Vancouver, BC V6T 2A3, Canada*
[4] *Department of Physics, Nagoya University, Nagoya 464-0814, Japan*
[5] *Frontier Research Institute for Interdisciplinary Sciences, and Cyclotron and Radioisotope Center, Tohoku University, Sendai, Miyagi 980-8578, Japan*

The MTV (Mott Polarimetry for T-Violation) experiment is running at TRIUMF-ISAC (Isotope Separator and ACcelerator), searching for a large T violation in polarized ^{8}Li β decay via measurements of the triple vector correlation, R, in the β decay rate function. The left/right backward scattering asymmetry of Mott scattering from a thin metal foil is measured using an electron tracking detector including a cylindrical drift chamber (CDC).

To achieve 10-ppm precision in the Mott scattering asymmetry, we performed multiple studies on the expected systematic effects. The sources of the systematics have been identified and calibration systems have been developed to evaluate the fake effects. The first physics data was collected in 2016 and significantly improved on the result of our previous measurement, which achieved 100-ppm precision in 2010 using the first generation detector (planer drift chamber) at TRIUMF. The data measurement status, together with the results of the systematics studies, is described here.

In addition to the T violation, we are preparing to test the Lorentz invariance in the weak sector via our Mott analyzer system. Unexplored Lorentz violating correlations can be tested using the MTV experimental setup. The testing principle and preparation status are also described here.

The 26th International Nuclear Physics Conference
11-16 September, 2016
Adelaide, Australia

*Speaker.

PoS(INPC2016)185

1. Introduction

It has been over a half century since the formalism of β decay was established. However, there are still unmeasured correlation coefficients [1, 2]. Of them, the two most interesting correlations are the D and R correlations, which violate time reversal symmetry [3, 4]. The β decay rate function expressed with all the possible correlations related to the electron spin can be expressed as

$$\begin{aligned}\omega \propto\ & 1+b\frac{m}{E_e}+\frac{\mathbf{p_e}}{E_e}\cdot\left(A\frac{<\mathbf{J}>}{J}+G\boldsymbol{\sigma}\right)\\ &+\boldsymbol{\sigma}\cdot\left[N\frac{<\mathbf{J}>}{J}+Q\frac{\mathbf{p_e}}{E_e+m}\left(\frac{<\mathbf{J}>}{J}\cdot\frac{\mathbf{p_e}}{E_e}\right)+R\frac{<\mathbf{J}>}{J}\times\frac{\mathbf{p_e}}{E_e}\right].\end{aligned} \tag{1.1}$$

When the electron's longitudinal polarization is not measured, one can ignore the related terms such that

$$\omega \propto 1+b\frac{m}{E_e}+A\frac{\mathbf{p_e}}{E_e}\cdot\frac{<\mathbf{J}>}{J}+N\boldsymbol{\sigma}\cdot\frac{<\mathbf{J}>}{J}+R\boldsymbol{\sigma}\cdot\left[\frac{<\mathbf{J}>}{J}\times\frac{\mathbf{p_e}}{E_e}\right]. \tag{1.2}$$

By defining the electron's velocity vector as $\boldsymbol{\beta_e}=\mathbf{p}_e/E_e$, and the nuclear polarization vector as $\mathbf{P}\equiv<\mathbf{J}>/J$, the rate function becomes

$$\omega \propto 1+A\boldsymbol{\beta}_e\cdot\mathbf{P}+N\boldsymbol{\sigma}\cdot\mathbf{P}+R\boldsymbol{\sigma}\cdot[\mathbf{P}\times\boldsymbol{\beta_e}]. \tag{1.3}$$

Here, the Fiertz interference term b is treated as negligibly small. The three correlations in Eq. (1.3), A, N, and R, are measured in our present study. In an experiment that is sensitive to the electron's transverse polarization, the measuring sensitivity is the analyzing power S. In real experiments using the Mott scattering as the transverse polarimeter, two additional parameters, ε (the detection efficiency) and S (the analyzing power of the Mott scattering), need to be included for the counting rate function n such that

$$n \propto \varepsilon\,(1+A\boldsymbol{\beta_e}\cdot\mathbf{P}+NS\boldsymbol{\sigma}\cdot\mathbf{P}+RS\boldsymbol{\sigma}\cdot[\mathbf{P}\times\boldsymbol{\beta_e}]). \tag{1.4}$$

The A correlation is measured as a well-known parity violating β anisotropy, which needs to be measured to determine the nuclear polarization P. Then, the leftward and rightward Mott scattering asymmetry will give the coefficients N and R.

2. The MTV experiment

The MTV experiment will measure the N and R correlations with the aim of detecting nonzero values for the first time in a nuclear system [5, 6]. With this as motivation, we investigate polarized ^{8}Li β decay, which is a pure Gamow-Teller transition. It is predicted that

$$N_{FSI} = -\gamma\frac{m}{E_e}A \tag{2.1}$$

$$R_{FSI} = -\frac{\alpha Zm}{p_e}A. \tag{2.2}$$

These are called final state interactions (FSIs). Indeed, R_{FSI} leads to a T violating observable. However, it does not violate time reversal symmetry. Our primary goal is to reach sufficient sensitivity to detect nonzero N_{FSI} and R_{FSI}. Precision measurements of N can probe the real part of the

expected new tensor interaction in weak decay. In addition, large R beyond the standard R_{FSI} will indicate the existence of an imaginary part of the new tensor interaction [7]. We aim to measure N and R at the same time. In this way, we can cancel the ambiguity in S by combining their results.

With this as motivation, we started the MTV experiment at TRIUMF-ISAC [8] using a highly polarized ^{8}Li beam. The polarized ^{8}Li beam is produced via the collinear laser optical pumping technique. The ^{8}Li beam, at approximately 30 keV, is stopped at our beam stopper foil (aluminum 10 μm). Then, the decayed electron exits the vacuum chamber, which is surrounded by a cylindrical Mott analyzer [9].

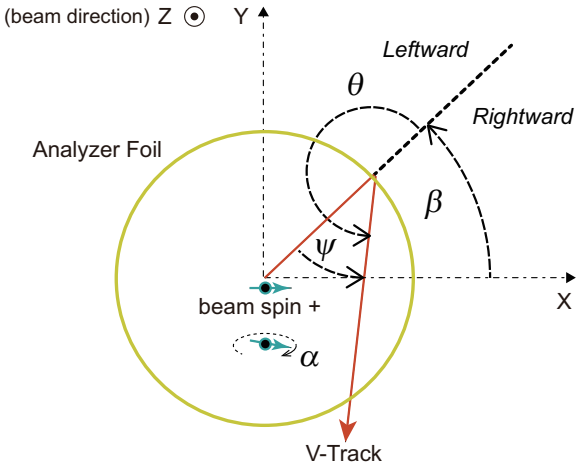

Figure 1: Coordinates of the MTV Mott analyzer using the CDC. The Mott scattering angle θ is defined as the scattering angle of the V-track. The electron's azimuthal emission angle β is defined as the angle from the beam spin direction in the spin + configuration [10]. If the beam spin polarization is not directed toward the X-axis, the rotation angle around the Y-axis is defined as α. The direction toward the Z-axis (the beam direction) corresponds to $\alpha = +\pi/2$.

As shown in Figure 1, the spin-polarized ^{8}Li beam is stopped at the beam stopper placed in the center of the cylindrical setup. Part of the emitted electrons is backwardly scattered from the cylindrical analyzer foil. The scattering tracks, called V-tracks, are detected using the cylindrical drift chamber (CDC). The electron's emitting angle β and the Mott scattering angle ψ are recorded event-by-event. Here, $\psi > 0$ ($\psi < 0$) is defined as rightward (leftward) Mott scattering. In addition, α is the rotation angle of the nuclear polarization around the Y-axis from the X-axis. The definition of the sign of α is shown in Figure 1. In ideal cases of nuclear spin, + (−) corresponds to $\alpha = 0$ ($\alpha = \pi$).

3. R and N correlations

Each event is recorded with its β and ψ angles. From this information, a counting number $N^{\pm}(\psi,\beta)$ is obtained for the beam spin ± cases. Using Eq. (1.4), the expected count rate is

$$N^{+}(\psi,\beta) \propto \int_{E_e}\int_{acceptance} \varepsilon\,(1 + A\boldsymbol{\beta_e}\cdot\mathbf{P} + NS\boldsymbol{\sigma}\cdot\mathbf{P} + RS\boldsymbol{\sigma}\cdot[\mathbf{P}\times\boldsymbol{\beta_e}])\,d\Omega dE_e. \tag{3.1}$$

In our case, the acceptance covers the $\pm\Delta z$ region along the axis direction of the cylindrical detector and small $\Delta\beta$. By calculating these geometrical correction factors, Eq. (3.1) can be re-written as

$$N^{+}(\psi,\beta) \propto \bar{\varepsilon}\left(1+Af_A\bar{\boldsymbol{\beta}}_e\cdot\mathbf{P}+Nf_N\bar{S}\boldsymbol{\sigma}\cdot\mathbf{P}+Rf_R\bar{S}\boldsymbol{\sigma}\cdot\left[\mathbf{P}\times\bar{\boldsymbol{\beta}}_e\right]\right), \tag{3.2}$$

using the mean efficiency $\bar{\varepsilon}$, the acceptance correction factors f_A, f_N, and f_R, and the mean $\bar{\boldsymbol{\beta}}_e = \boldsymbol{\beta}_e/|\beta_e| \times <\beta_e>$. For each case of beam spin $\pm$ and leftward (rightward) Mott scattering $\psi<0$ ($\psi>0$),

$$\begin{aligned}
N^{+}(\psi<0,\beta) &\propto \bar{\varepsilon}(\psi,\beta)\left(1+Af_A\bar{\boldsymbol{\beta}}_e\cdot\mathbf{P}+Nf_N\bar{S}\boldsymbol{\sigma}\cdot\mathbf{P}+Rf_R\bar{S}\boldsymbol{\sigma}\cdot\left[\mathbf{P}\times\bar{\boldsymbol{\beta}}_e\right]\right)\\
N^{+}(\psi>0,\beta) &\propto \bar{\varepsilon}(\psi,\beta)\left(1+Af_A\bar{\boldsymbol{\beta}}_e\cdot\mathbf{P}-Nf_N\bar{S}\boldsymbol{\sigma}\cdot\mathbf{P}-Rf_R\bar{S}\boldsymbol{\sigma}\cdot\left[\mathbf{P}\times\bar{\boldsymbol{\beta}}_e\right]\right)\\
N^{-}(\psi<0,\beta) &\propto \bar{\varepsilon}(\psi,\beta)\left(1-Af_A\bar{\boldsymbol{\beta}}_e\cdot\mathbf{P}-Nf_N\bar{S}\boldsymbol{\sigma}\cdot\mathbf{P}-Rf_R\bar{S}\boldsymbol{\sigma}\cdot\left[\mathbf{P}\times\bar{\boldsymbol{\beta}}_e\right]\right)\\
N^{-}(\psi>0,\beta) &\propto \bar{\varepsilon}(\psi,\beta)\left(1-Af_A\bar{\boldsymbol{\beta}}_e\cdot\mathbf{P}+Nf_N\bar{S}\boldsymbol{\sigma}\cdot\mathbf{P}+Rf_R\bar{S}\boldsymbol{\sigma}\cdot\left[\mathbf{P}\times\bar{\boldsymbol{\beta}}_e\right]\right).
\end{aligned} \tag{3.3}$$

Then, the conventional double ratio can be defined as

$$\begin{aligned}
D(\psi,\beta) &\equiv \frac{N^{+}(\psi<0,\beta)}{N^{+}(\psi>0,\beta)}\frac{N^{-}(\psi>0,\beta)}{N^{-}(\psi<0,\beta)}\\
&= \frac{\left(1+Af_A\bar{\beta}_eP\cos\alpha\cos\beta+N\bar{S}P\sin\alpha+Rf_R\bar{S}\bar{\beta}_eP\cos\alpha\sin\beta\right)}{\left(1+Af_A\bar{\beta}_eP\cos\alpha\cos\beta-N\bar{S}P\sin\alpha-Rf_R\bar{S}\bar{\beta}_eP\cos\alpha\sin\beta\right)}\\
&\times \frac{\left(1-Af_A\bar{\beta}_eP\cos\alpha\cos\beta+N\bar{S}P\sin\alpha+Rf_R\bar{S}\bar{\beta}_eP\cos\alpha\sin\beta\right)}{\left(1-Af_A\bar{\beta}_eP\cos\alpha\cos\beta-N\bar{S}P\sin\alpha-Rf_R\bar{S}\bar{\beta}_eP\cos\alpha\sin\beta\right)}\\
&\equiv \frac{\left(1+\hat{A}\cos\beta+\hat{N}+\hat{R}\sin\beta\right)}{\left(1+\hat{A}\cos\beta-\hat{N}-\hat{R}\sin\beta\right)}\times\frac{\left(1-\hat{A}\cos\beta+\hat{N}+\hat{R}\sin\beta\right)}{\left(1-\hat{A}\cos\beta-\hat{N}-\hat{R}\sin\beta\right)}\\
&= 1+\frac{4(\hat{N}+\hat{R}\sin\beta)}{1-(\hat{A}\cos\beta)^2}-\cdots\quad(\hat{N},\hat{R}<<1)\\
&= 1+4(\hat{N}+\hat{R}\sin\beta).\quad(\hat{A}<<1)
\end{aligned} \tag{3.4}$$

From Eq. (3.4), it is clear that deviation from $D=1$ implies a non-zero $\hat{N}$ as a constant component and $\hat{R}$ as a sine-curve component as a function of β. Usually, asymmetry is used instead of D such that

$$A_{sym}(\psi,\beta) \equiv \frac{\sqrt{D}-1}{\sqrt{D}+1} \sim \hat{N}+\hat{R}\sin\beta. \tag{3.5}$$

The expected signal is shown in Figure 2.

4. Systematic Effects on R

The efficiency inhomogeneity can be canceled in the double ratio analysis via beam spin flipping. In our previous studies, we recognized two major systematic effects that cannot be canceled using this beam spin flipping technique. The source of these systematics is the parity violating A correlation. The parity violating β anisotropy flips with the beam spin flipping. As of 2015, we had found two types of systematics.

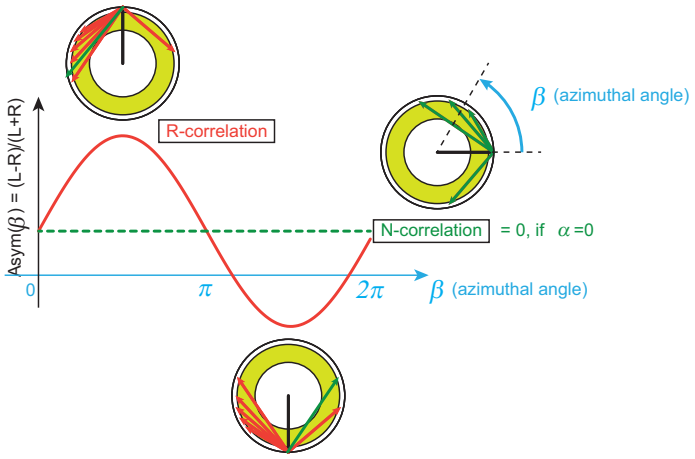

Figure 2: Expected signal of N and R on a A_{sym} versus β plot.

- Type 1. $A_{sym} > 0$ at $\beta = \pi/2$
- Type 2. $A_{sym} < 0$ at $\beta = \pi/2$

Their properties are shown in our previous report [10]. In 2016, we performed an intensive study of this systematic effect by studying: [A] the source position dependence, [B] the beam polarization dependence, [C] the coincidence window dependence, and [D] the beam intensity dependence.

In Figure 3, typical values of A_{sym} are plotted as a function of β. We integrated $N(\psi,\beta)$ over ψ in our present analysis. Therefore, the effective analyzing power $\bar{S}$ needs to be estimated under the ψ integration. The region around $\beta \sim \pi/2$ is empty because we removed the analyzer foil in this region to estimate the foil ON/OFF effects, such as the signal to noise ratio. The events observed in the foil OFF configuration are not thought to originate from Mott scattering on the analyzer foil. Therefore, such events reduce the analyzing power. We estimate the effective analyzing power $\bar{S}$ by including the acceptance correction and this noise contribution effect.

The Type-I systematic shows a clear dependence on the width of the coincidence window. This strongly suggests that this effect results from an accidental coincidence. If a couple of straight tracks from two different β decay events is recognized as a V-Track, such an effect must increase as a function of the coincidence window width. Because the accidental hit rate is increased with the radiation intensity, this effect is synchronized with the parity violating β anisotropy. The $(\sin\beta)$ shape observed in Figure 3 is understood as being this effect. It is also confirmed that this effect increases with the beam intensity, which is consistent with our interpretation.

To study this Type-I effect without using a real spin polarized beam, we developed a linear robot calibration system to simulate parity violating β anisotropy. In this case, the detector setup constantly changes the location, oscillating in the $\pm$ X direction. The Type-I effect was confirmed for the robot calibration system and for the polarized beam test in 2016.

As for the Type-2 effect, a source intensity dependence was not clearly observed. The coincidence window dependence cannot easily be estimated independently from the Type-I effect. Recently, we concluded that this Type-2 effect has neither a coincidence window dependence nor a source intensity dependence. Our previous interpretation of this effect was the gain reduction of the

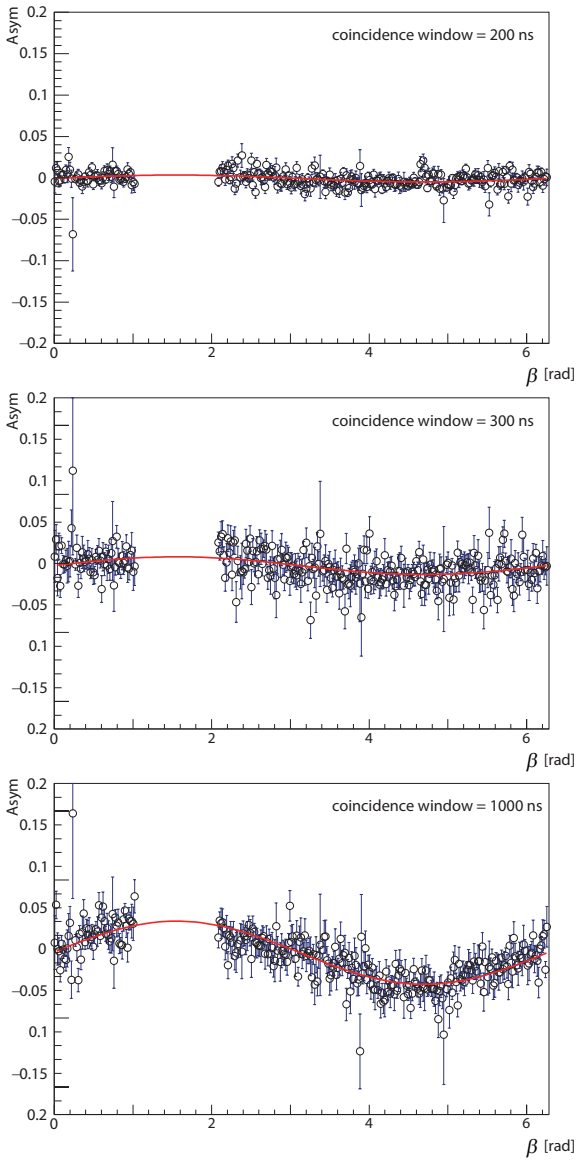

Figure 3: Typical plot of A_{sym} versus β for the coincidence windows (top) 200 ns, (middle) 300 ns, and (bottom) 1000 ns.

detector [10], which should, however, show a beam intensity dependence. Currently, we believe that this is simply a geometrical effect due to changing the scattering angle. The changing of the scattering angle leads to a change in the scattering cross section; therefore, this effect should not show a beam intensity dependence.

In a real experiment, the Type-2 effect does not exist, unless we artificially change the detector position synchronized with the beam spin flipping. The robot calibration system was believed to be effective in estimating all the parity violation related systematics. However, we must conclude that this assumption was not correct. The robot system causes an additional Type-2 effect, which does not exist in the real measurement. Therefore, we built a different systematics evaluation system for

the Type-1 effect. The accidental hit effect for the spin $\pm$ can be treated as

$$\varepsilon(\psi,\beta) \to \varepsilon(\psi,\beta)(1+\delta^{\pm}(\beta)),$$

by adding the contribution of the efficiency from the accidental hits. This additional term $\delta^{\pm}$ cannot be canceled by the conventional double ratio technique because $\delta^{\pm}$ is not constant over spin flipping. Instead, we measure A_{asym} as a function of the coincidence window width and the beam intensity. A typical result is shown in Figure 4. This figure shows a clear scaling to these two factors, which is consistent with the interpretation of accidental coincidence.

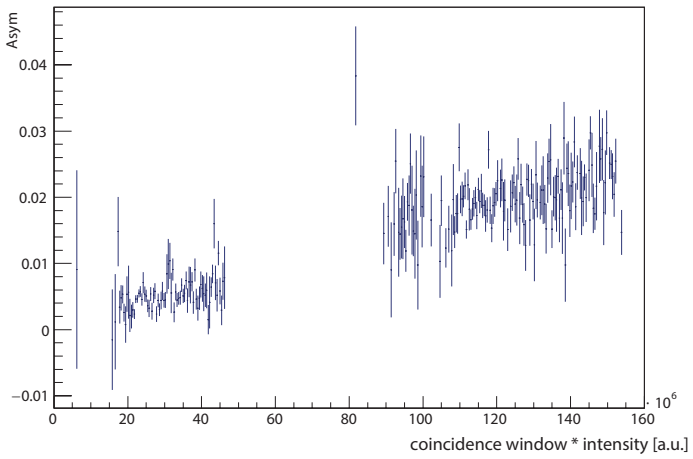

Figure 4: Typical plot of the sine-curve amplitude of $A_{sym}(\beta)$ versus the coincidence window $\times$ intensity.

5. Measurement of N

At our original experimental setup, $\alpha = 0$. the contribution from the N correlation is zero. To produce $\alpha \neq 0$, we installed a new rotational table system to rotate the detector setup. The configuration with $\alpha \neq 0$ produces a beam longitudinal polarization $P_L = P_Z = P \sin\alpha$ and a transverse polarization $P_T = P_X = P\cos\alpha$. The change in α is observed as a change in the offset component of $A_{asym}(\beta)$ apart from the sine component. The setup is shown in Figure 5. The systematic effects originate from the parity violation. Therefore, there is no such effect on the constant component. The contribution from the R and N contributions is obtained at the same time by the $A_{sym}(\beta)$ fitting with the same order of statistical precision.

The N correlation is useful to check the calculation of the effective analyzing power $\bar{S}$, which is common with the R measurement. In addition, the measurement of the N correlation itself can test the existence of a real part of the unknown tensor interaction.

6. Lorentz Violation and Solar Neutrinos

Apart from the physics of the R or N correlations in conventional β decay formalism [1], the MTV experiment can probe other physics that require time-varying properties of the weak interaction. For example, it has been pointed out that the MTV is sensitive to unmeasured correlations in

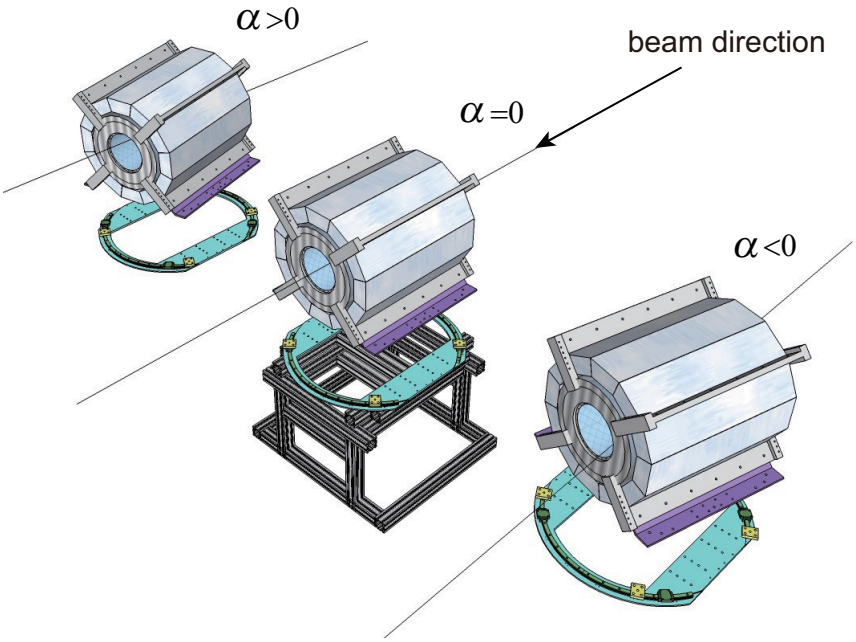

Figure 5: New rotational table system to produce nonzero α for the N correlation measurement.

the $\chi_{\mu\nu}$ framework, which is proposed as a set of Lorentz violating coefficients [11]:

$$\omega \propto 1 - \frac{2}{3}\chi_r^{00} + \frac{2}{3}(\chi_r^{l0} + \tilde{\chi}_i^l)\boldsymbol{\beta}_e^l - \frac{1}{3}[(1-\chi_r^{00})\boldsymbol{\beta}_e \cdot \mathbf{P} + \tilde{\chi}_i^l \mathrm{P}^l + \chi^{lk}\beta_e^l P^k + \boldsymbol{\chi}_i^{0l} \cdot (\boldsymbol{\beta}_e \times \mathbf{P})^l]. \quad (6.1)$$

The new coefficients, χ's, are the proposed new Lorentz violating coefficients. The last term can be tested as a siderian variation of $(\boldsymbol{\beta}_e \times \mathbf{P})$. In our case, the electron's emission direction $\boldsymbol{\beta}_e$ about $\mathbf{P}$ should be measured as a time sequence. We can also measure the lifetime difference of ^{8}Li between the spin $+$ and $-$ cases as a time sequence. This is similar to the work at KVI [12]. The MTV experiment is sensitive to the term $\tilde{\chi}_i^l \mathrm{P}^l$. If day variation in the lifetime asymmetry over the spin $\pm$

$$A_\tau = \frac{\tau^+ - \tau^-}{\tau^+ + \tau-} \quad (6.2)$$

is observed, it means that there is a special direction $\tilde{\chi}_i^l$ in the weak interaction. It may be possible to test not only the Lorentz violation but also Solar neutrino-related phenomena [13] using this measurement.

Even though it is not included in (6.1), it is also possible to examine the variation of σ, which requires our Mott analyzer. In addition, to perform long-term calibration measurements using an unpolarized source, the term $\frac{2}{3}(\chi_r^{l0} + \tilde{\chi}_i^l)\boldsymbol{\beta}_e^l$ can be tested.

7. Experimental Status

In 2016, we performed the first physics production run using the current CDC setup. The observed accidental effect was confirmed as consistent with the Type-1 effect, which is well understood and controlled. The expected statistical and systematic precision was approximately

A_{asym} ∼100-ppm over the two days of data production. The physics interpretation of R and N in the 2016 dataset will be published soon. Data production is also scheduled in and after 2017, when we will reach a precision of A_{asym} ∼10-ppm. In the 2016 dataset, we performed a measurement of the lifetime asymmetry A_τ as the daily (sidereal) variation with a precision of 100-ppm. Other Lorentz violation observables are also recorded. The analysis results will be reported soon.

References

[1] J. D. Jackson, S. B. Treiman, and H. W. Wyld, Jr., Phys. Rev (1957) 517; Nucl. Phys. 4 (1957) 206.

[2] N. Severijns, M. Beck, and O. Naviliat-Cuncic, Rev. Mod. Phys. 78, (2006) 991.

[3] J. Sromicki *et al.*, Phys. Rev. Lett. 82 (1999) 57.

[4] R. Huber *et al.*, Phys. Rev. Lett. 90 (2003) 202301.

[5] J. Murata *et al.*, EPJ Web of Conf. 66 (2014) 05017.

[6] J. Murata *et al.*, Hyperfine Interact. 225, (2014) 193-196.

[7] N. Yamanaka *et al.*, J. High Energy Phys. 2014, 12 (2014) 1-54.

[8] C.D.P. Levy, *et al.*. Nucl. Instrum. Meth. B204, (2003) 689-693.

[9] S. Tanaka *et al.*, Nucl. Instrum. Meth. A752 (2014) 47-53.

[10] J. Murata *et al.*, Hyperfine Interact (2016) 237:12.

[11] J.P. Noordmans, H.W. Wilschut, and R.G.E. Timmermans, Phys. Rev. C 87, 055502 (2013).

[12] S. E. Muller *et al.*, Phys. Rev. D **88**, 071901 (2013).

[13] P.A. Sturrock, E. Fischbach, J.D. Scargle, Solar Physics, 291, (2016) 3467.